Journal of Solid State Chemistry **160,** 388–393 (2001)
doi:10.1006/jssc.2001.9252, available online at http://www.idealibrary.com on IDEAL®

Microstructural Evolution of Electrochemically Cycled Si-Doped SnO_2–Lithium Thin-Film Battery

Young-Il Kim, C. S. Yoon,[1] and J. W. Park

Division of Materials Science and Engineering, Hanyang University, Seoul, 133-791, Korea

Received January 25, 2001; in revised form May 10, 2001; accepted May 25, 2001; published online July 16, 2001

SnO_2 and Si-doped SnO_2 thin-film electrodes were deposited on a Mo/Si substrate with an e-beam evaporator at room temperature. In the voltage range of 0.1–0.8 V, a reversible capacity of 400 mAh/g was attained after 200 cycles with the Si doping whereas the pure SnO_2 exhibited a much faster capacity fade. Transmission electron microscopy (TEM) revealed that Si has segregated to form a Sn–Si solid solution after the first discharge. After subsequent cycling, the tin particles in the Si-doped film were observed to break up in contrast to the particle growth observed in the pure film. TEM study indicated that Si in the tin particles forms a stable amorphous layer whereas in the pure SnO_2, recrystallization of the amorphous material is believed to occur. TEM study showed that there were important differences in the microstructure, which could be responsible for the improvement of the Si addition on the cycling performance.

Key Words: **tin oxide; electrochemical cycling; anode; lithium battery; reversible capacity fade.**

1. INTRODUCTION

Since Fuji Photo Film Co. reported that tin oxide is a promising alternative anode material for the lithium secondary battery (1), a great research effort has been dedicated to replacing the existing graphite-based anodes. To optimize the performance of the material, tin oxide has been introduced in a number of different forms ranging from ultrafine alloy powders such as $SiSnO_3$, Li_2SnO_3 (2), mechanically alloyed Sn–Fe(–C) powders (3), nanocrystalline SnSb (4), and NiSi and FeSi alloy powders (5). Tin oxide has been also prepared as a thin film for potential use as the anode material for the rechargeable microbattery system (6–8), serving as an independent power supply for micromachining and a backup source for electronic circuits.

Despite high theoretical gravimetric and volumetric capacities for tin oxide, the formation of metallic Sn and Li_2O during the first cycle brings about a large irreversible capacity loss and a substantial volume change in the material (9). In addition to the initial loss, the volume differences between Li–Sn alloy and Sn in subsequent cycling are known to cause gradual capacity loss and eventually destroy the mechanical integrity of the material (6, 9). Great effort has been spent to minimize such dimensional instability of the Sn electrodes and it was concluded that the microstructure of the tin oxide has an important effect on the cycling behavior of the material (10).

In our work, we have prepared Si-doped SnO_2 thin films using e-beam evaporation at room temperature to study the effects of Si on the microstructure of tin oxide electrodes. Si, being a strong glass-making agent and having the ability to form a Li–Si alloy (5), is expected to have a strong impact on the cycling performance. In fact, we have observed that the Si addition has substantially reduced the capacity fade typically observed in the material and the maximum improvement was attained at 5 mol % addition of Si. In this paper, we have utilized transmission electron microscopy to discern the reasons for such improvement by comparing the microstructure of the pure SnO_2 and 5 mol % Si-doped SnO_2 thin-film electrodes at various stages of electrochemical cycling.

2. EXPERIMENTAL DETAILS

Nanocrystalline Si-doped SnO_2 films were deposited on a Mo/Si substrate using an e-beam evaporator at room temperature. The powder source was produced by grinding a mixture of reagent grade SnO_2 and 5 mol % Si (99.95% purity, Cerac Co., USA) and cold-pressing the powder mixture into disks at 2 kPa. Prior to the tin oxide film deposition, Mo current collector thin films with thickness of 2500 Å were predeposited onto a boron-doped p-type Si(100) substrate by metal sputtering (400 W, 5 mTorr). On top of the Mo film, a 1200-Å-thick tin oxide film is deposited using the e-beam evaporator. The thicknesses of the two films were calibrated using cross-sectional transmission electron microscopy (XTEM). XTEM showed that both

[1]To whom correspondence should be addressed. E-mail: csyoon@email.hanyang.ac.kr. Fax: 82-2-2290-1838.

0022-4596/01 $35.00

films were continuous, free of pinholes. To calculate the film mass of SnO_2, an assumed density of 6.95 g/cm^3 was used (11).

For the electrochemical cycling, a cell was assembled with Li foil as the counter and reference electrodes and 1 M $LiPF_6$–ethylene carbonate (EC)/dimethyl carbonate (DMC) (1:1 by volume) as the electrolyte. Galvanostatic charge–discharge tests were performed with a constant current of 100 μA/cm^2-μm from 0.1 to 0.8 V vs Li/Li^+.

The Surface morphology of the film after the electrochemical cycling was observed with a field emission scanning electron microscope (JSM-6330F, JEOL, Japan) (SEM) and the microstructure was characterized using a transmission electron microscope (JEM-2010, JEOL, Japan) (TEM). The composition of the film was verified using energy-dispersive X-ray spectroscopy (EDS). In order to preserve the film microstructure and to minimize the degradation of the cycled films during TEM specimen preparation, the films were kept in ethanol and the backside of the film was ground away in ethanol for ion milling. One-sided ion milling to the backside of the film was done using a liquid-nitrogen-cooled stage to minimize the damage to the involved phases during milling.

3. RESULTS AND DISCUSSION

Figure 1 shows the electrochemical cycling behavior of the tin oxide thin film with and without Si doping|Li foil cell when cycled between 0.1 V and 0.8 V. The large drop in the discharge capacity after the first cycle, which is typically observed for the tin oxide electrode, has been attributed to the first-order phase transformation related to the formation of Li_2O and the subsequent reduction of the SnO_2 during the lithium insertion. After the first cycle, the Si-doped SnO_2 electrode exhibited a maximum capacity of 600 mAh/g which gradually dropped to 400 mAh/g over 200 cycles while the reversible capacity of the pure SnO_2 thin-film electrode reached 200 mAh/g at the end of 200 cycles despite the slower drop in capacity during the first 30 cycles. The addition of Si substantially improved the discharge capacity of the tin oxide electrode as the Si appears to stabilize the electrochemical behavior over an extended cycling period.

Shown in Fig. 2a is the TEM image of the tin oxide film after the first discharge showing the metallic tin crystal formed shown through the reduction of SnO_2 by Li. The electron diffraction pattern indicated that the crystal was β-Sn with tetragonal structure with $a = 3.2$ Å and $c = 5.8$ Å, which was surrounded by an amorphous matrix. Figure 2b shows a number of tin grains that have agglomerated to form a polycrystalline material. The initial irreversible reaction that produced the observed tin crystals and the reversible electrochemical reaction during subsequent cycles are given below (10):

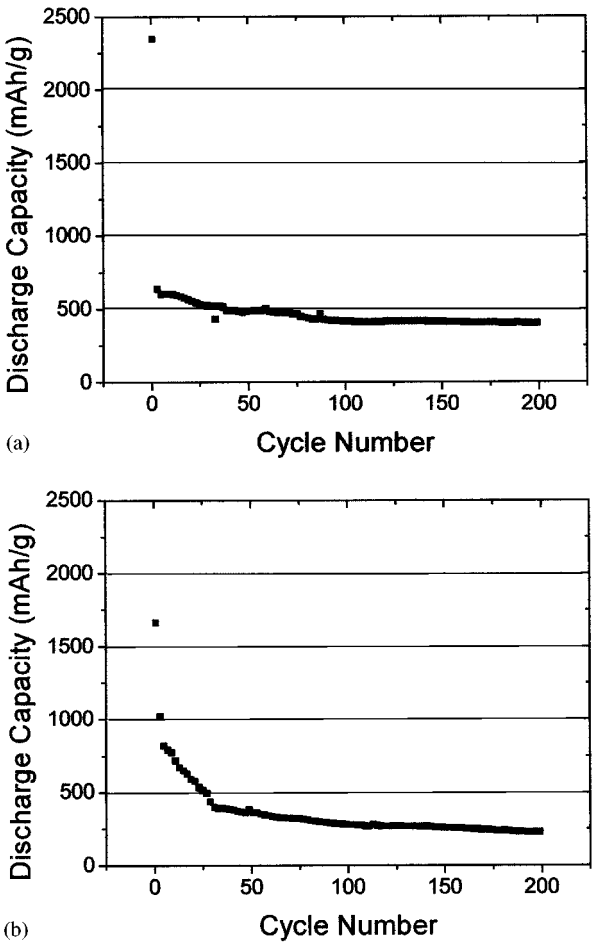

FIG. 1. Charge–discharge curves of SnO_2 film when cycled from 0.1 V to 0.8 V: (a) 5 mol% Si-doped SnO_2 film, (b) pure SnO_2 film.

$$SnO_2 + 4Li \rightarrow Sn + 2Li_2O \text{ (after 1st cycle)} \quad [1]$$

$$mSn + nLi \leftrightarrow Li_nSn_m \text{ (during cycling).} \quad [2]$$

To find how Si is distributed in the film after the first discharge, the concentration profile of Si across the tin crystal is measured as shown in Fig. 2c. It can be seen that the tin crystal was enriched with Si compared to the surrounding amorphous lithium oxide matrix. The Si enrichment is rather surprising because Sn–Si does not show any solid solubility below 230°C as evidenced in the Sn–Si binary phase diagram (12).

From the thermodynamic point, Si in SnO_2 should be reduced together with SnO_2 through the following reaction:

$$SiO_2 + 4Li \rightarrow Si + 2Li_2O. \quad [3]$$

Since the Gibbs free energy of formation of Li_2O at 25°C is -561 kJ/mol and -802 kJ/mol for SiO_2 (13), the

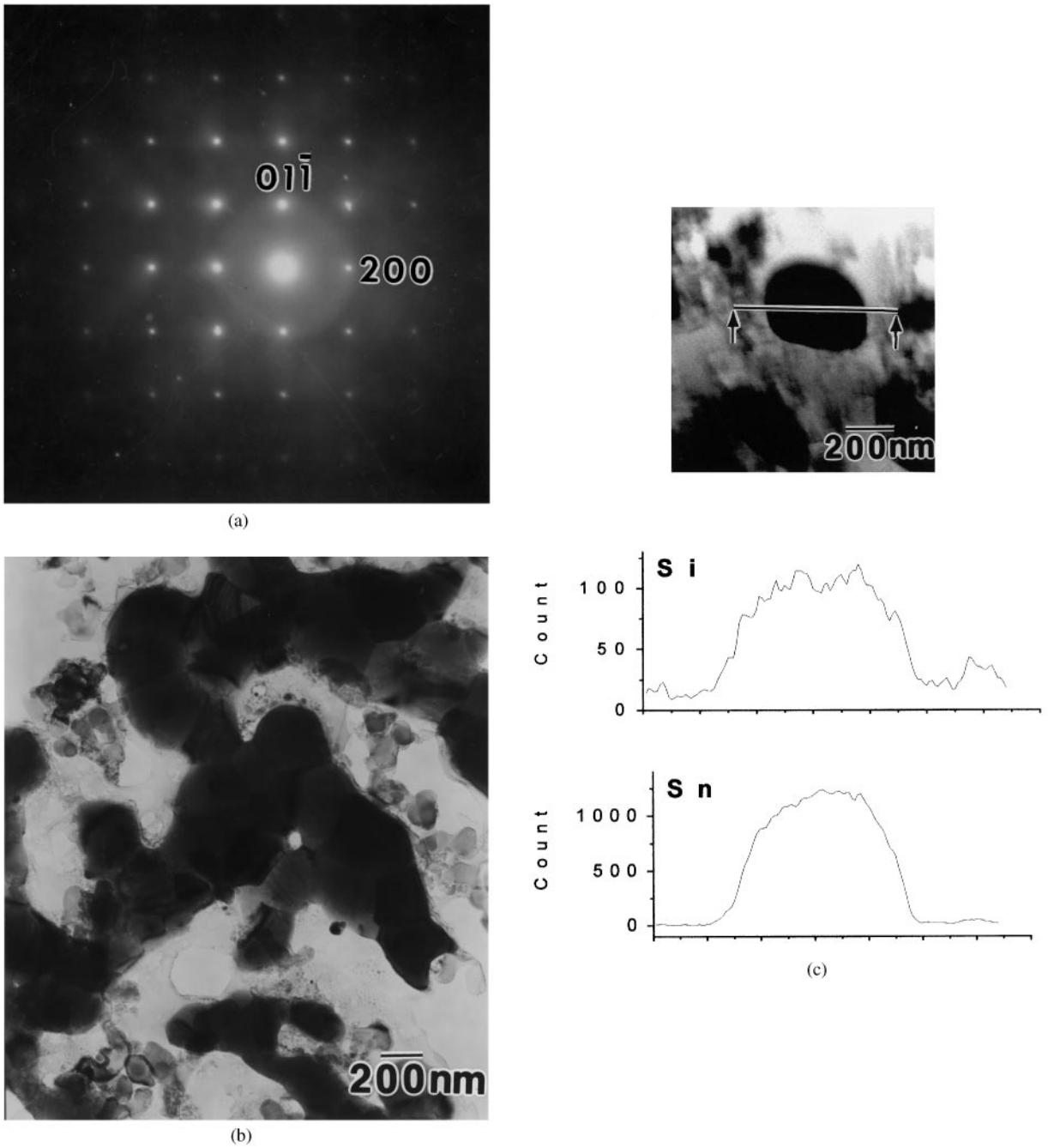

FIG. 2. TEM images of 5 mol% Si-doped SnO_2 film after the first discharge: (a) tin single crystal with the electron diffraction pattern in [011] zone, (b) polycrystalline aggregate of tin crystals, (c) EDS compositional line scan across a tin crystal.

reaction should proceed. However, SiO_2, composed of strong Si–O bonds, is a stable network-forming oxide. It is unlikely that Li is able to break all the Si–O bonds to reduce the oxide while SnO_2 is a less stable oxide with a Gibbs formation energy of -520 kJ/mol [also evidenced by comparing the bond strength of two oxides, $SiO_2 = 106$ kcal/mol, $SnO_2 = 46$ kcal/mol (14)] and readily reduced by Li. Furthermore, there is experimental evidence that Si will exist as SiO_2 and Li_2SiO_3, which was confirmed through IR spectroscopy, when $Sn_{1-x}Si_xO_2$ anode|Li is electrochemically cycled (15). Therefore, it is not clear why Si remained in the SnO_2 film to form a nonequilibrium phase, Sn–Si solid solution in this case.

Figure 3 shows the pure tin grains after the first charge upon which lithium is extracted from the SnO_2 film. As can be seen in Fig. 3a, the grain size of tin crystals has become

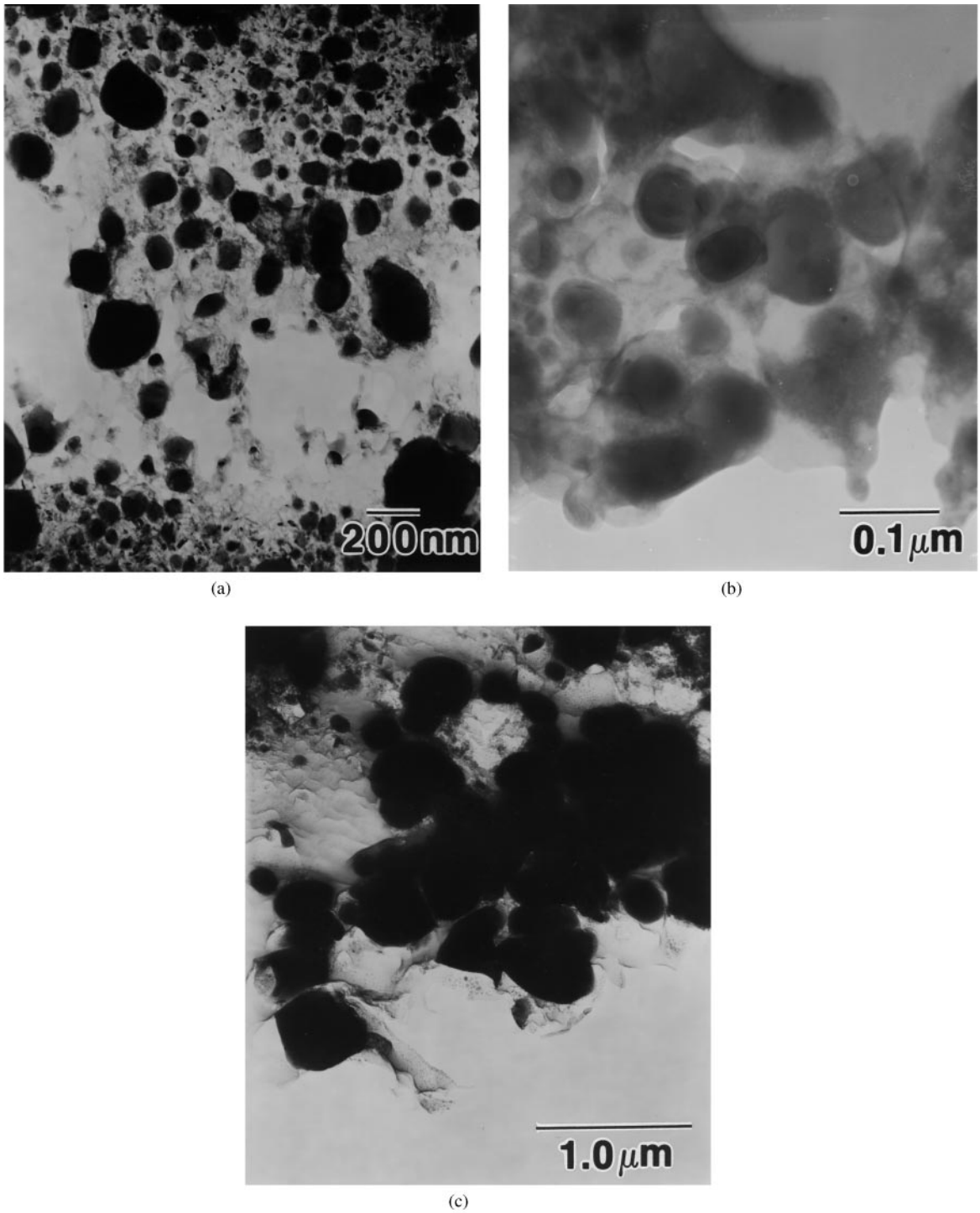

FIG. 3. TEM images of 5 mol% Si-doped SnO_2 film after the first charge cycle: (a) tin crystals with decreased particle size, (b) magnified image of tin particles surrounded by a layer of amorphous material, (c) a large polycrystalline aggregate breaking up into smaller particles after the first charge cycle.

considerably smaller which was also evidenced by the scanning electron microscope (SEM) observation of a huge volume reduction of the thin film upon lithium extraction. In fact, we have observed through SEM that after the first charge, the thickness of the tin oxide film reduced to 30% of the thickness after the first lithium insertion cycle. In Fig. 3b, the small tin grains are magnified to show the amorphous layer encircling the tin crystals. As pointed by Retoux *et al.*

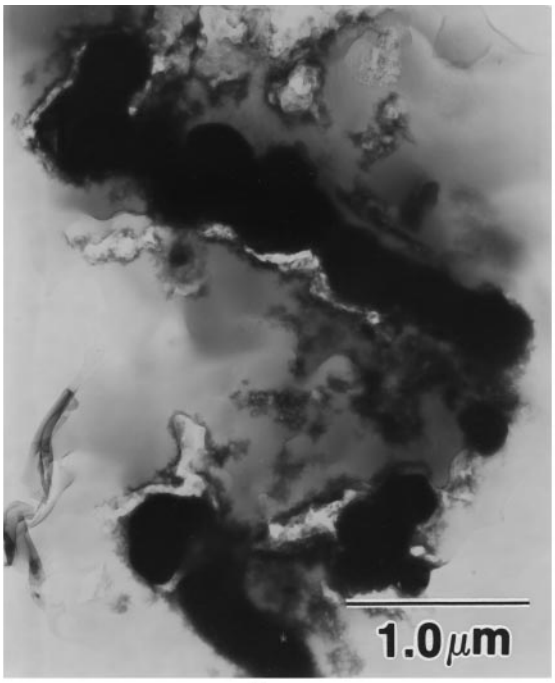

(a)

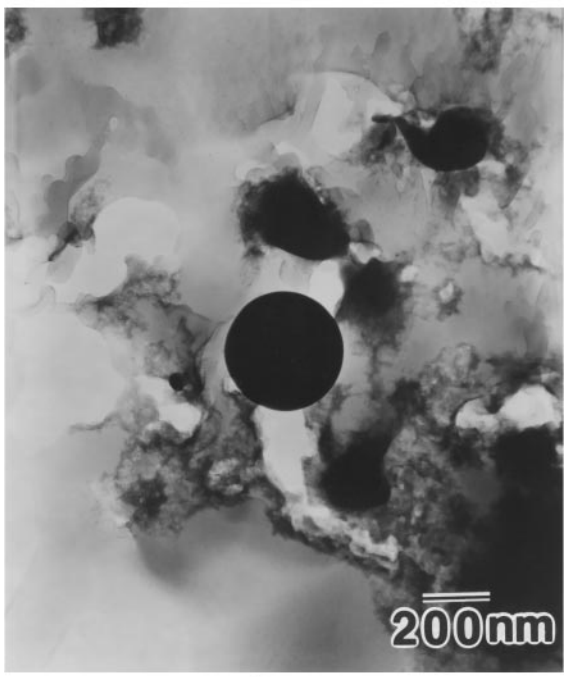

(b)

FIG. 4. TEM images of 5 mol% Si-doped SnO_2 film after the second charge cycle: (a) a large polycrystalline aggregate breaking up into smaller circular particles after the second charge cycle due to the Raleigh shape instability, (b) perfectly round tin particle separated from a larger aggregate.

in their TEM study (16), the tin grains were surrounded by a thin layer of amorphous material composed of tin, oxygen, and silicon as confirmed by EDX. It can be also seen in Fig. 3c that a polycrystalline agglomeration of tin crystals as observed in Fig. 2b breaks up into individual particles upon lithium extraction. From the micrographs, it can be conjectured that the excess oxygen generated by the lithium extraction has reoxidized the particles to form

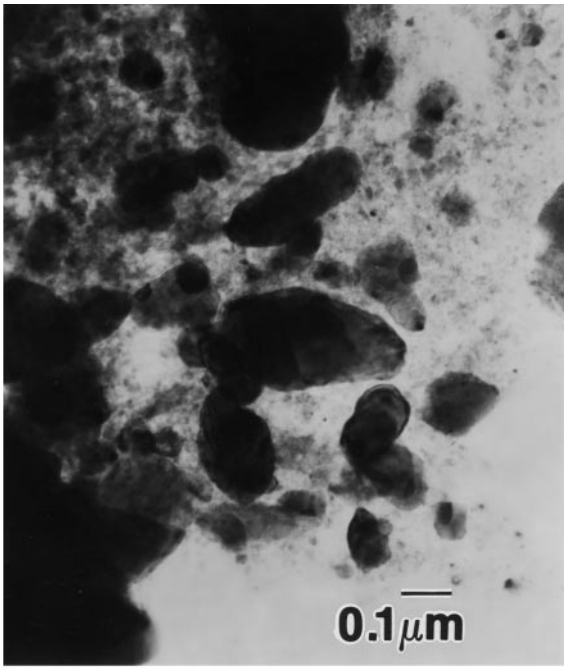

(a)

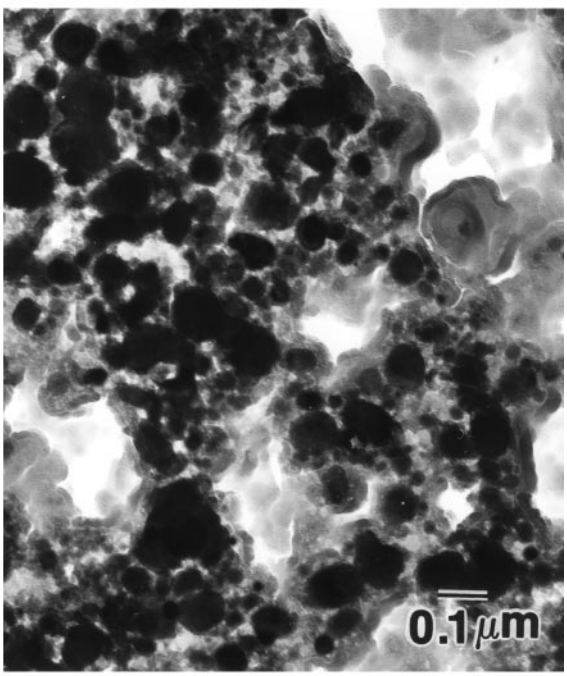

(b)

FIG. 5. TEM images of the SnO_2 film after the 200 cycles: (a) the pure SnO_2 film, (b) 5 mol% Si-doped SnO_2 film, demonstrating the difference in the final particle size.

a stable amorphous surface oxide based on a Sn–Si–O network. In case of the polycrystalline agglomeration, oxygen atoms have been preferentially transported through the grain boundary to create an oxide layer along the grain boundary, which leads to an eventual breaking-up of the particles.

The TEM images of the SnO_2 film in subsequent charge–discharge cycles clearly show the morphological changes undergone by the tin particles. Figure 4 shows the Si-doped SnO_2 film after the second charge cycle. Shown in Fig. 4a is clear evidence of the large tin particles being broken up into smaller circular particles upon cycling. A perfectly round particle that has been separated from the larger particle is shown in Fig. 4b. The large particles of metastable Sn–Si solid solution formed during the first discharge cycle appear to become unstable with respect to the electrochemical cycling and the particles break into discrete circular particles which is very similar to the phase break-up caused by the Rayleigh shape instability (17). Such particle separation was not observed in the pure SnO_2 film in our study. Neither was such an observation made in their TEM work on the pure SnO_2 electrodes done by Retoux *et al*. (16). Courtney and Dahn have, in fact, concluded that the Li–Sn alloy formation induces tin atoms to aggregate into clusters and repeated cycling causes growth of the tin particles in the pure SnO_2 electrodes (2). Our TEM observation clearly demonstrated that the 5% Si addition has greatly altered the microstructure of the SnO_2 thin film in response to the electrochemical cycling.

Shown in Figs. 5a and 5b are the TEM images of the pure and Si-doped SnO_2 films after 200 cycles. It can be clearly seen that the particle size is much smaller in the Si-doped SnO_2 electrode after 200 cycles. The improvement of reversible capacity due to the Si addition can be attributed to the prevention of the tin particle growth which is believed to be the main reason for the capacity fade for the pure SnO_2 electrodes through the loss of electrical contact.

We have also found a layer of amorphous material based on a Sn–Si–O network surrounding the tin particles. Although the role of the amorphous layer on the electrochemical properties is not exactly known, it has been suggested that the crystallization of the layer is related to the degradation of the cell capacity (16). Following the suggestion, the presence of Si in the amorphous network would make the amorphous layer less susceptible to the crystallization as Si atoms are much stronger network formers compared to Sn atoms, which is evidenced by the bond strength of the two oxides. It is reasonable to assume that surface oxidation of the Si-enriched tin particles was also partially responsible for the improvement in the cell performance of the Si-doped SnO_2 thin films.

4. CONCLUSION

We have demonstrated that Si doping of the SnO_2 thin film deposited at room temperature significantly retards the reversible capacity fade typically observed from the pure SnO_2 films during electrochemical cycling. TEM observation combined with compositional analysis has revealed that the tin particles formed through reduction by Li during the first discharge was enriched in Si compared to the surrounding amorphous matrix. The tin particles were also surrounded by a thin layer of amorphous material based on a Sn–Si–O network. From our observation, we have concluded that the Si enrichment has retarded the tin particle growth and recrystallization of the amorphous surface oxide to enhance the cycle performance of the material.

REFERENCES

1. J. H. Kennedy, *Thin Solid Film* **43,** 41 (1997).
2. I. A. Courtney and J. R. Dahn, *J. Electrochem. Soc.* **144,** 2943 (1997).
3. O. Mao, R. A. Dunlap, and J. R. Dahn, *J. Electrochem. Soc.* **146**(2), 405 (1999).
4. J. O. Besenhard, M. Wachtler, M. Winter, R. Andreaus, I. Rom, and W. Sitte, *J. Power Sources* **81–82,** 268 (1999).
5. G. X. Wang, L. Sun, D. H. Bradhurst, S. Zhong, S. X. Dou, and H. K. Liu, *J. Power Sources* **88,** 278 (2000).
6. T. Brousse, R. Retoux, U. Herterich, and D. M. Schleich, *J. Electrochem. Soc.* **145**(1), 1 (1998).
7. F. Ding, Z. Fu, M. Zhou, and Q. Qin, *J. Electrochem. Soc.* **146**(10), 3554 (1999).
8. W. H. Lee, H. C. Son, H. S. Moon, Y. I. Kim, S. H. Sang, J. Y. Kim, J. G. Lee, and J. W. Park, *J. Power Sources* **89,** 102 (2000).
9. I. A. Courtney and J. R. Dahn, *J. Electrochem. Soc.* **144,** 2045 (1997).
10. H. Li, X. Huang, and L. Chen, *J. Power Sources* **81–82,** 335 (1999).
11. "Handbook of Physics and Chemistry, 73rd ed." (D. R. Lide, Ed.), CRC Press, Boca Raton, FL, 1992.
12. P. V. Chevalier, Thermodata SGTE report (1986) at http://www.met.kth.se/pd.
13. "The Oxide Handbook, 2nd ed." (G. V. Samsonov, Ed.), p. 45, IFI/Plenum, New York, 1982.
14. L. H. van Vlack, "Physical Ceramics for Engineers," p. 62, Addison-Wesley, Reading, MA, 1964.
15. H. Huang, E. M. Kelder, L. Chen, and J. Schoonman, *J. Power Sources* **81–82,** 362 (1990).
16. R. Retoux, T. Brouse, and D. M. Schleich, *J. Electrochem. Soc.* **146**(7), 2472 (1999).
17. M. Chiang, D. Birnie, and W. D. Kingery, "Physical Ceramics," p. 368, Wiley, New York, 1997.